

## Supporting Information

Oxygenated functional group-engaged electroless deposition of ligand-free silver nanoparticles on porous carbon for efficient electrochemical non-enzymatic H<sub>2</sub>O<sub>2</sub> detection

Qian Chen,<sup>a</sup> Lingxi Zhou,<sup>b</sup> Weidong Jiang,<sup>c,\*</sup> and Guangyin Fan<sup>a,\*</sup>

<sup>a</sup> College of Chemistry and Materials Science, Sichuan Normal University, Chengdu 610068, China.

<sup>b</sup> State Key Laboratory of New Ceramics and Fine Processing, School of Materials Science and Engineering, Tsinghua University, Beijing 100084, China.

<sup>c</sup> School of Chemistry and Environmental Engineering, Sichuan University of Science & Engineering, Zigong 643000, China.

\* Corresponding author

Email: jwdx@sicnu.edu.cn (W.D. Jiang); fanguangyin@sicnu.edu.cn (G.Y. Fan).

The file includes Experimental Section, Figs. S1-S15 and Tables S1-S4.

## **Chemical and materials**

Potassium citrate ( $C_6H_5K_3O_7$ ), sodium chloride (NaCl), fructose (Fru), urea (Urea), uric acid (UA), ascorbic acid (AA), sucrose (Suc) and silver nitrate ( $AgNO_3$ ) were obtained from Aladdin Industrial Inc., China. Nafion (5 wt%) was supplied by Sigma-Aldrich. Graphene oxide was purchased from Nanjing XFNANO Materials Tech Co., Ltd.  $K_2HPO_4 \cdot 3H_2O$ ,  $KH_2PO_4 \cdot 3H_2O$ , and  $H_2O_2$  were purchased from Chengdu Kelong Reagent Co., Ltd. Different kinds of milk, including Mengniu/250 mL (milk-M, Inner Mongolia), Ely/250 mL (milk-E, Inner Mongolia) and Trenwith/250 mL (milk-T, Inner Mongolia), and orange juices, such as Master Kong/250 mL (juice-M, Tianjin), President/500 mL (juice-P, Shanghai) and Coca/500 mL (juice-C, Shanghai) were purchased from Wal-Mart supermarket, China. Bovine serum obtained from Shanghai Hyclone. All of the above chemicals were of analytical grade and used without further purification. De-ionized (DI) water was used for preparing samples. Double distilled water was used throughout the electrochemical measurement.

**Syntheses of PC:** Typically, 1.5 g potassium citrate was calcined in a tube furnace under argon at 800 °C for 1 h<sup>1</sup>. The resulting solid was rinsed by an aqueous HCl solution (1.0 M) for 24 h. Subsequently, the black powder was isolated through centrifugation, washed with water, and dried at 70 °C for 10 h.

## **Characterization**

X-ray diffraction (XRD) was recorded using a Rigaku D/Max-2500 (Rigaku Co., Japan) diffractometer with a Cu K $\alpha$  radiation to determine the crystal structure. The

morphologies of the obtained samples were characterized using a scanning electron microscope (SEM) (FE-SEM, JSM-7500, Japan) and a transmission electron microscopy (TEM) (JEM-2100F, JEOL, Japan). X-ray photoelectron spectroscopy (XPS) spectra and ultraviolet photoelectron spectrum (UPS) were recorded on a Thermo ESCALAB 250 Axis Ultra spectrometer (VG Scientific, UK) using an Al K $\alpha$  radiation. Fourier transform infrared spectroscopy (FTIR) spectrum was performed on NEXUS 670 infrared spectrophotometer (Thermo Nicolet, USA). The spectrum was recorded in the range from 400 to 4000 cm<sup>-1</sup> by using pressed KBr tables. Inductively coupled plasma-atomic emission spectrometry (ICP-AES) analysis was carried out on SPECTRO ARCOS spectrometer. The Brunauer–Emmett–Teller (BET) surface area and pore volume of the samples was analyzed by an ASAP 2020 Micromeritics instrument.

## The calculation of $\Delta E$

The driving force for the SIED is the positive  $\Delta E$  between the reduction potential of

$\text{Ag}^+$  ( $\varphi_{\text{Ag}^+}/\varphi_{\text{Ag}}$ ) and the oxidation potential of PC ( $\varphi_{\text{R - PC/O - PC}}$ ). According to Eq. (1), the value of  $\Delta E$  can be calculated. The oxidation potential of  $\varphi_{\text{R - PC/O - PC}}$  was calculated to be -0.25 V on the basis of the work function from the UPS result.

Additionally, the reduction potential of  $\varphi_{\text{Ag}^+}/\varphi_{\text{Ag}}$  was calculated to be 0.779 V according to the Nernst equation Eq. (2). Therefore, the value of  $\Delta E$  was calculated to be 1.029 V, indicating that the spontaneous redox reaction for the synthesis of Ag/PC was thermodynamically feasible.

$$\Delta E = \varphi_{\text{Ag}^+}/\varphi_{\text{Ag}} - \varphi_{\text{R - PC/O - PC}} \quad (1)$$

$$\varphi_{\text{Ag}^+}/\varphi_{\text{Ag}} = 0.779 + \frac{0.059}{1} \log \frac{[\text{Ag}^+]}{[\text{Ag}]} \quad (2)$$

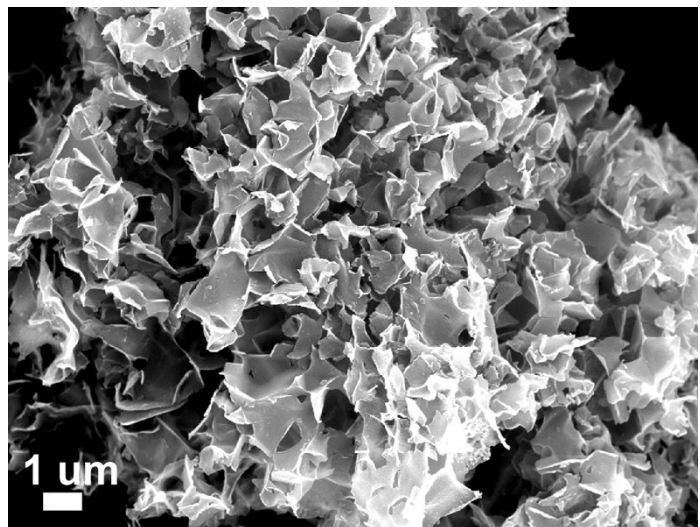


**Fig. S1** Low-magnification SEM image.

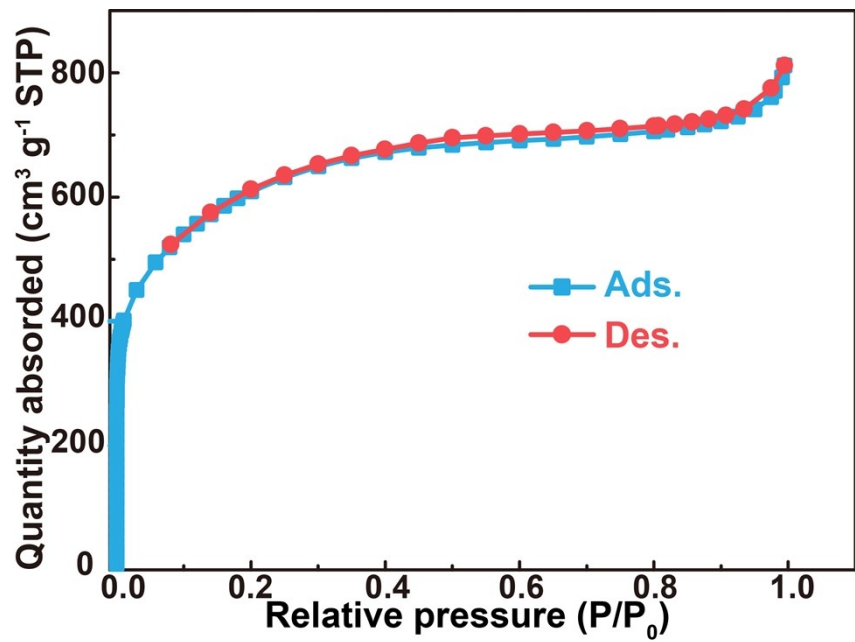


**Fig. S2**  $N_2$  sorption isotherm curve of PC.

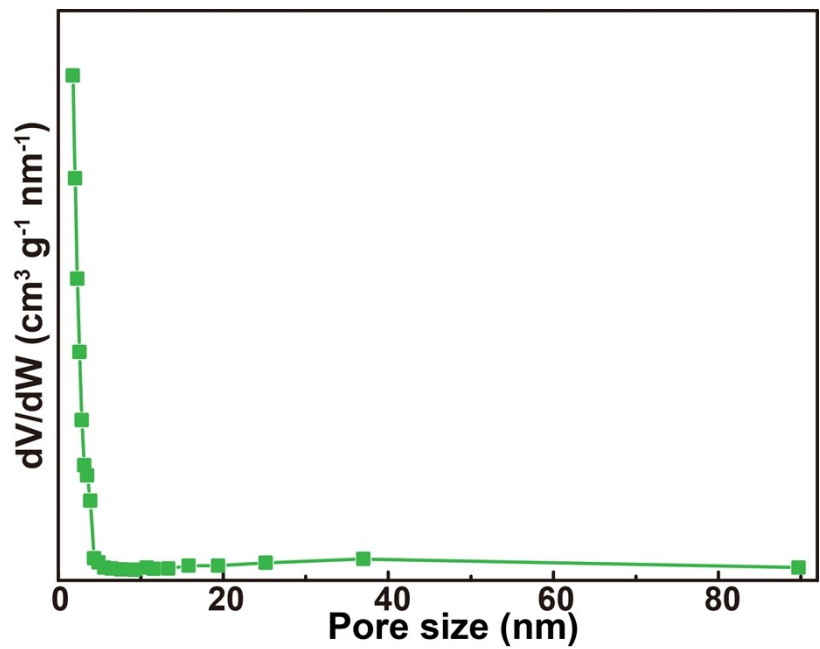


**Fig. S3** The pore size distribution of PC.

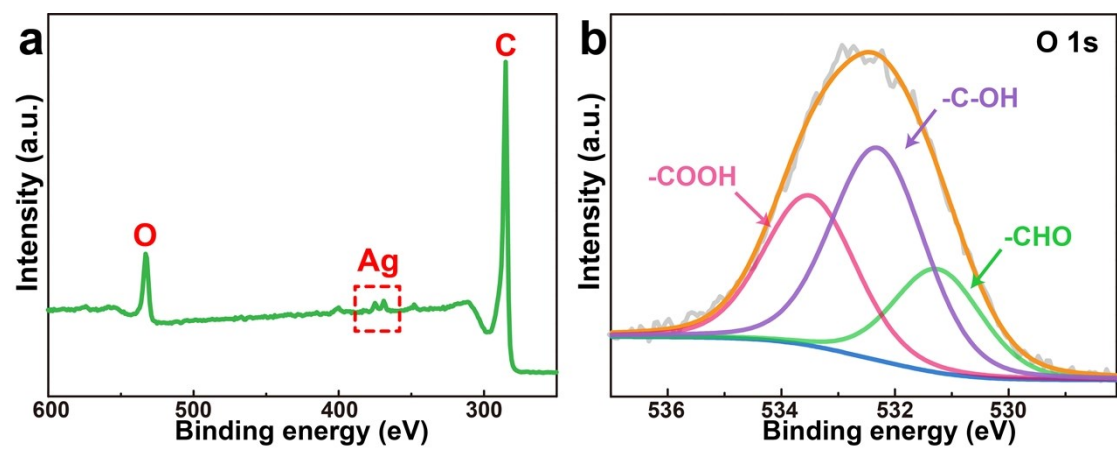


**Fig. S4** (a) XPS full scan spectra and (b) O 1s high resolution XPS spectra for Ag/PC-6.

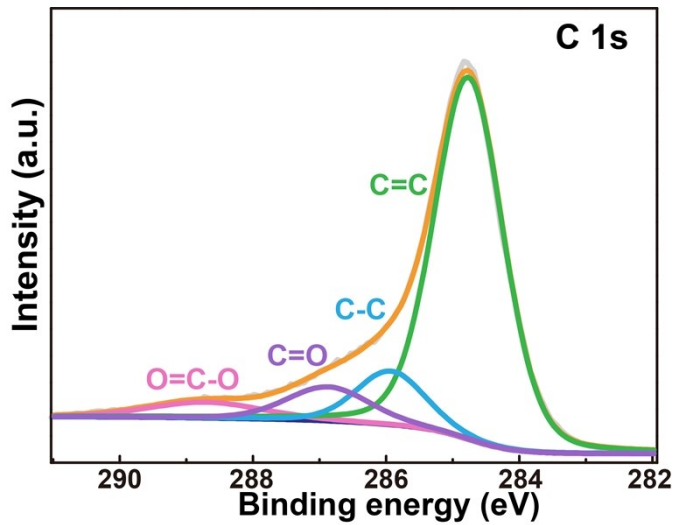


**Fig. S5** C1s high resolution XPS spectra for Ag/PC-6.

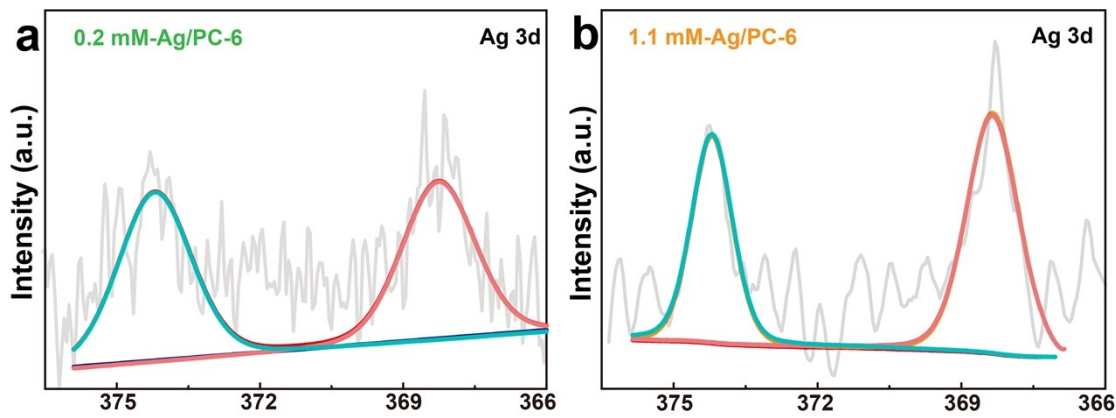


**Fig. S6** Ag 3d high resolution XPS spectra for 0.2 mM-Ag/PC-6 (a) and. 1.1 mM-Ag/PC-6 (b).

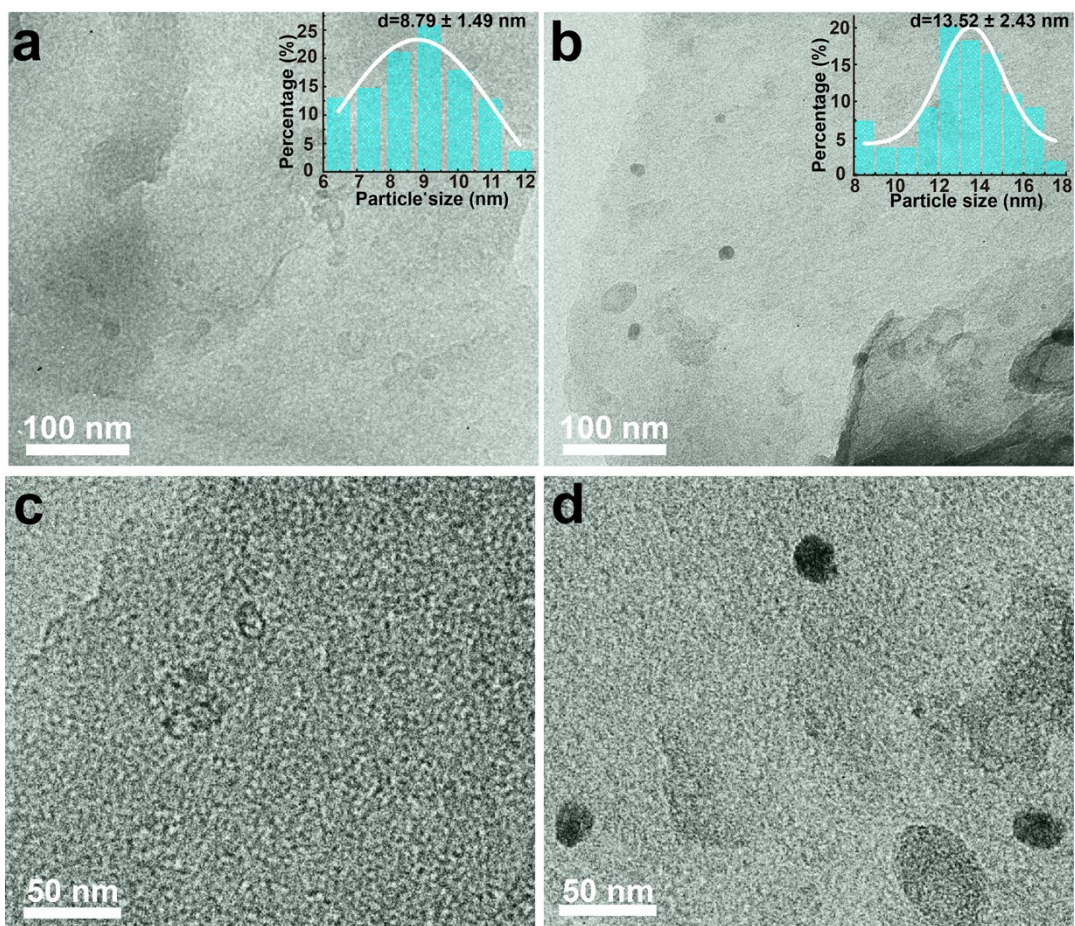


**Fig. S7** TEM images of 0.2 mM-Ag/PC-6 (a, c) and 1.1 mM-Ag/PC-6 (b, d).

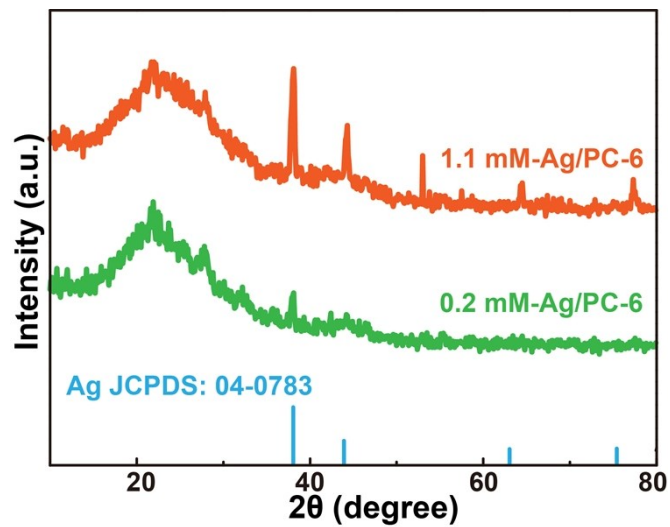


**Fig. S8** XRD patterns of 1.1 mM-Ag/PC-6 and 0.2 mM-Ag/PC-6.

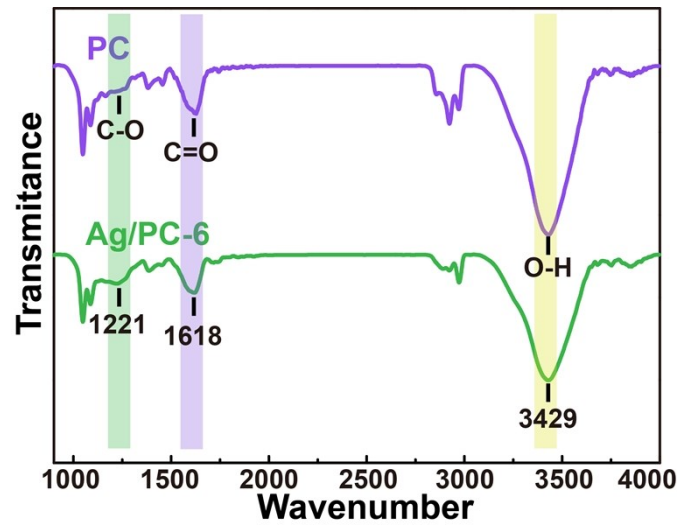


**Fig. S9** The FTIR characterization of PC and Ag/PC-6.

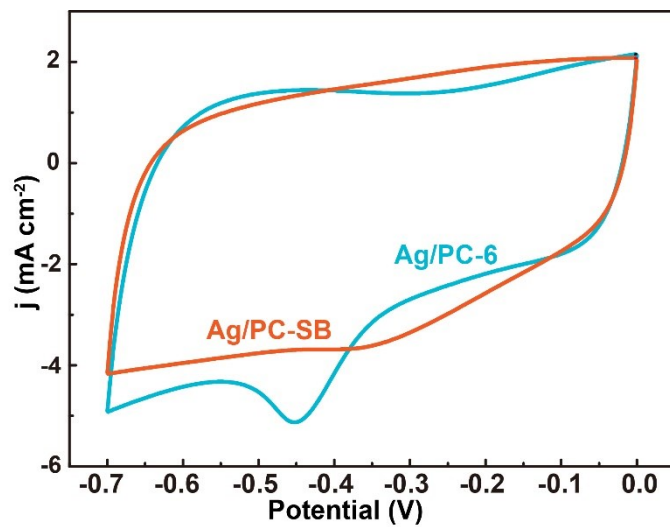


**Fig. S10** CVs of Ag/PC-6 and Ag/PC-SB in 0.1 M PBS with 5 mM  $\text{H}_2\text{O}_2$  (Scan rate: 50 mV s<sup>-1</sup>).

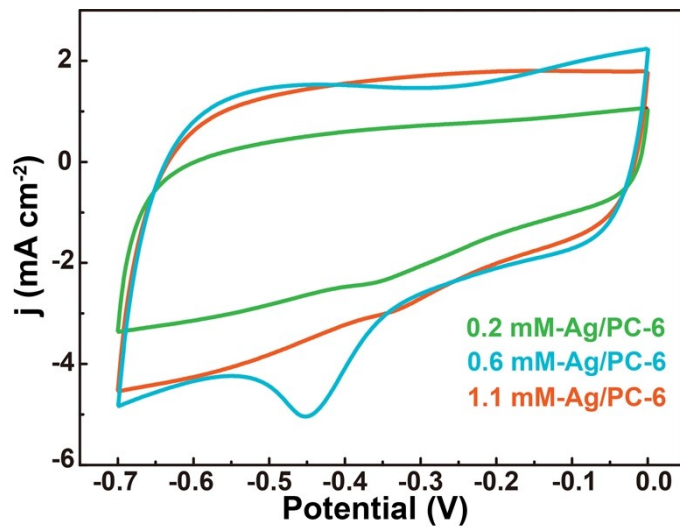


**Fig. S11** CVs of Ag/PC-6 with different Ag ions concentration (0.2, 0.6 and 1.1 mM) in 0.1 M PBS in the presence of 5 mM H<sub>2</sub>O<sub>2</sub> (Scan rate: 50 mV s<sup>-1</sup>).

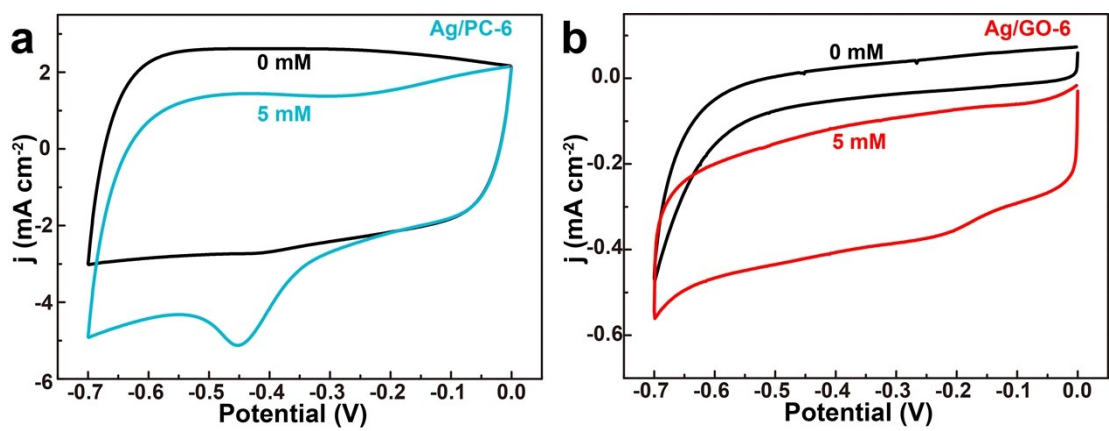


**Fig. S12** CVs of Ag/PC-6 (a) and Ag/GO-6 (b) in 0.1 M PBS in the absence and presence of 5 mM H<sub>2</sub>O<sub>2</sub> (Scan rate: 50 mV s<sup>-1</sup>).

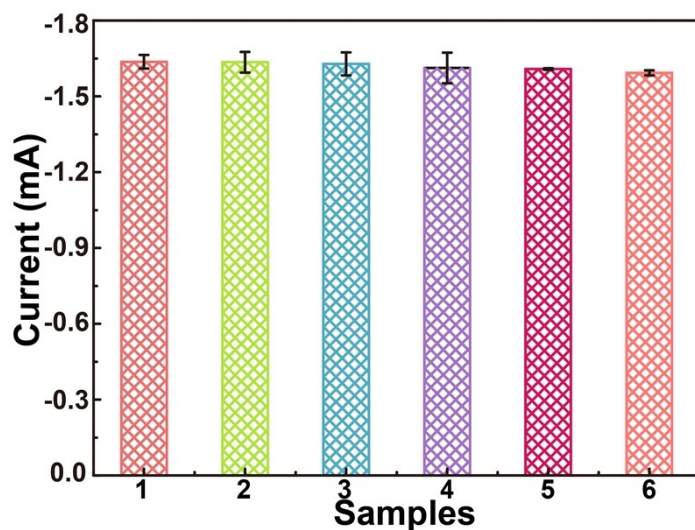


**Fig. S13** Cathodic peak currents of the six successive tests with the same Ag/PC-6 in 9 mM H<sub>2</sub>O<sub>2</sub> (n=3).

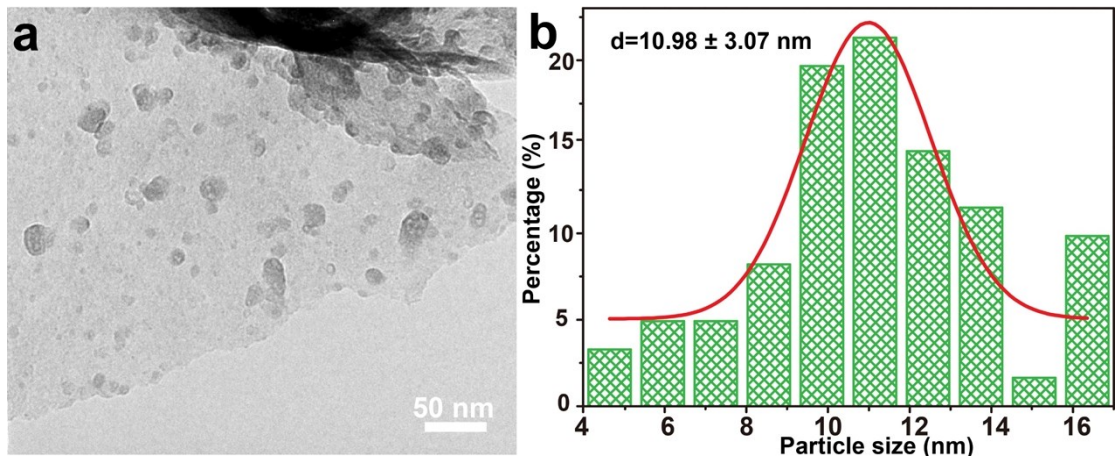
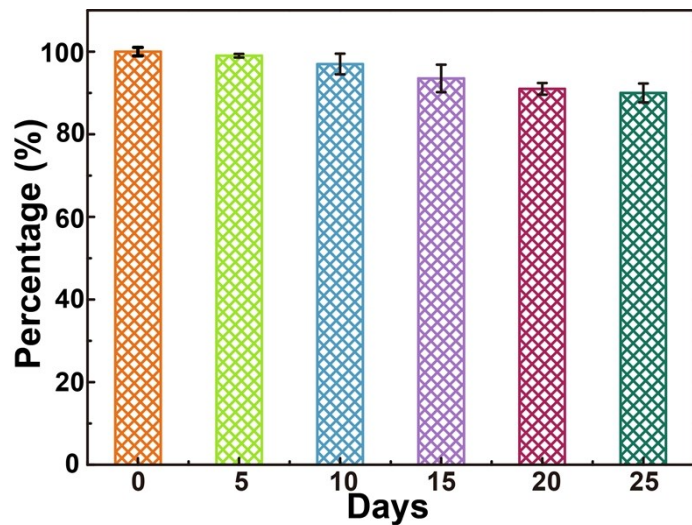


Fig. S14 TEM image (a) and the particle size distribution (b) of Ag/PC-6 after the electrochemical H<sub>2</sub>O<sub>2</sub> detection about 5000s.



**Fig. S15** Six tests with same Ag/PC-6 electrode to H<sub>2</sub>O<sub>2</sub> monitoring in 25 days (n=3).

**Table S1.** ICP characterization results of Ag/PC-1, Ag/PC-6, and Ag/PC-10.

Materials	Ag NPs content by ICP (wt%)
Ag/PC-1	0.91
Ag/PC-6	1.24
Ag/PC-10	1.28

**Table S2.** XPS characterization results of PC and Ag/PC-6.

Materials	O element content <sup>a</sup> (at%)	-C-OH group content (at%)	-CHO group content (at%)
PC	13.42	7.1	3.2
Ag/PC-6	10.58	4.8	1.9

<sup>a</sup> The content of Co element is collected by full scan spectrum of XPS.

**Table S3.** Comparison of electrochemical performance of previous reported sensors for H<sub>2</sub>O<sub>2</sub> detection.

Electrodes	Linear range (mM)	LOD ( $\mu\text{M}$ )	Sensitivity ( $\mu\text{A mM}^{-1} \text{ cm}^{-2}$ )	Refs.
Ag NPs/porous silicon	0.0016-0.5	0.45	-	2
Ag NS/ITO	0.2-4	1	-	3
Ag NPs/3DG	0.03-16.21	16.21	-	4
Ag NPs/DNA	0.004-16	1.7	-	5
AgNPs/GN/GCE	0.1-40	28	-	6
Ag/MnO/CNTs/GC E	0.005-10.4	1.7	82.5	7
LSG-Ag	0.100-10	7.9	-	8
Inkjet printed Ag electrode	0.1 - 6.8	5.0	287	9
Ag/NCNFs	0.020–20	0.15	142.2	10
Cu <sub>2</sub> O/AuCu/Cu	0.010-9	0.14	127.98	11
Au@Ag@C	0.005-4.75	0.14	-	12
AgCo/MWCNT/G CE	-	0.74	57.14	13
N-graphene-Ag NDs/ITO	0.1 - 80	0.26	88.47	14
Ag nanosheets	0.005-6	0.17	320.3	15

Ag–HNTs–MnO <sub>2</sub>	0.002-4.71	0.7	119	<sup>16</sup>
Au-SiO <sub>2</sub> -MTs	0.01-1	0.6	-	<sup>17</sup>
Pt-N-graphene/ITO	0.001-1	0.34	61.23	<sup>18</sup>
Pt-PVA-CNT/GCE	0.002–3.8	0.7	122.63	<sup>19</sup>
ZnO <sub>3</sub> -CuO <sub>7</sub> /CPE	0.003-0.53	2.4	1.11	<sup>20</sup>
PdCu/CB nanohybrid	0.0004-5.0	0.054	-	<sup>21</sup>
AuPd@GR	0.005-11.5	1	186.86	<sup>22</sup>
Mn@FeNi-S/GO	-	0.0088	8.929	<sup>23</sup>
Co@MOF-808	0.01-0.45	1.3	382.27	<sup>24</sup>
CC/Co@C-CNTs	0.0004-7.2	0.27	388	<sup>25</sup>
Nanorough Ag layer	0.01-22.5	6	-	<sup>26</sup>
AgNPs-rGO	0.1-60	1.8	-	<sup>27</sup>
MWCNT/Ag	0.05-17	0.5	1.42	<sup>28</sup>
Ag nanowire	0.1-3.1	29.2	266	<sup>29</sup>
<b>Ag NP/PC-6</b>	<b>0.001-20</b>	<b>0.729</b>	<b>226.9</b>	<b>This work</b>

---

**Table S4.** Real-time detection of H<sub>2</sub>O<sub>2</sub> in real samples.

Food Samples	Added (μM)	Recovery rates (%)	
		n=3	RSD (%)
juice-M	10	91.2	1.6
juice-P	10	96.0	2.1
juice-C	10	90.6	5.4
milk-M	10	86.4	3.5
milk-E	10	97.0	2.9
milk-T	10	80.0	2.2
scrum	10	99.0	2.0

## References

1. M. Sevilla and A. B. Fuertes, *ACS Nano*, 2014, **8**, 5069-5078.
2. A. A. Ensafi, F. Rezaloo and B. Rezaei, *Sens. Actuators, B* 2016, **231**, 239-244.
3. M. Amiri, S. Nouhi and Y. Azizian-Kalandaragh, *Mater. Chem. Phys.*, 2015, **155**, 129-135.
4. B. Zhan, C. Liu, H. Shi, C. Li, L. Wang, W. Huang and X. Dong, *Appl. Phys. Lett.*, 2014, **104**, 243704.
5. K. Cui, Y. Song, Y. Yao, Z. Huang and L. Wang, *Electrochim. Commun.*, 2008, **10**, 663-667.
6. L. Jia, J. Liu and H. Wang, *Electrochim. Acta* 2013, **111**, 411-418.
7. Y. Han, J. Zheng and S. Dong, *Electrochim. Acta* 2013, **90**, 35-43.
8. E. Aparicio-Martínez, A. Ibarra, I. A. Estrada-Moreno, V. Osuna and R. B. Dominguez, *Sens. Actuators, B* 2019, **301**, 127101.
9. L. Shi, M. Layani, X. Cai, H. Zhao, S. Magdassi and M. Lan, *Sens. Actuators, B* 2018, **256**, 938-945.
10. H. Guan, Y. Liu, Z. Bai, J. Zhang, S. Yuan and B. Zhang, *Mater. Chem. Phys.*, 2018, **213**, 335-342.
11. X. Liang, W. Li, H. Han and Z. Ma, *J. Electroanal. Chem.*, 2019, **834**, 43-48.
12. Y. Li, Y. Zhang, Y. Zhong and S. Li, *Appl. Surf. Sci.*, 2015, **347**, 428-434.
13. H. C. Kazici, F. Salman, A. Caglar, H. Kivrak and N. Aktas, *Fuller. Nanotube Car. N.*, 2018, **26**, 145-151.
14. M. T. Tajabadi, W. J. Basirun, F. Lorestani, R. Zakaria, S. Baradaran, Y. M. Amin, M. R. Mahmoudian, M. Rezayi and M. Sookhakian, *Electrochim. Acta* 2015, **151**, 126-133.
15. B. Ma, C. Kong, X. Hu, K. Liu, Q. Huang, J. Lv, W. Lu, X. Zhang, Z. Yang and S. Yang, *Biosens. Bioelectron.*, 2018, **106**, 29-36.
16. S. Zhang, Q. Sheng and J. Zheng, *RSC Adv.*, 2015, **5**, 26878-26885.
17. S. Liu, B. Yu, F. Li, Y. Ji and T. Zhang, *Electrochim. Acta*, 2014, **141**, 161-166.
18. M. T. Tajabadi, M. Sookhakian, E. Zalnezhad, G. H. Yoon, A. M. S. Hamouda, M. Azarang, W. J. Basirun and Y. Alias, *Appl. Surf. Sci.*, 2016, **386**, 418-426.
19. Y. Fang, D. Zhang, X. Qin, Z. Miao, S. Takahashi, J.-i. Anzai and Q. Chen, *Electrochim. Acta* 2012, **70**, 266-271.
20. S. Daemi, S. Ghasemi and A. Akbar Ashkarraan, *J. Colloid Interface Sci.*, 2019, **550**, 180-189.
21. Y. Liu, H. Li, S. Gong, Y. Chen, R. Xie, Q. Wu, J. Tao, F. Meng and P. Zhao, *Sens. Actuators, B* 2019, **290**, 249-257.
22. T. D. Thanh, J. Balamurugan, S. H. Lee, N. H. Kim and J. H. Lee, *Biosens. Bioelectron.*, 2016, **85**, 669-678.
23. S. Manavalan, J. Ganesamurthi, S.-M. Chen, P. Veerakumar and K. Murugan, *Nanoscale*, 2020, **12**, 5961-5972.
24. Y.-S. Chang, J.-H. Li, Y.-C. Chen, W. H. Ho, Y.-D. Song and C.-W. Kung, *Electrochim. Acta*, 2020, **347**, 136276.
25. L. Long, H. Liu, X. Liu, L. Chen, S. Wang, C. Liu, S. Dong and J. Jia, *Sens. Actuators, B* 2020, **318**, 128242.
26. W. Lian, L. Wang, Y. Song, H. Yuan, S. Zhao, P. Li and L. Chen, *Electrochim. Acta*, 2009, **54**, 4334-4339.
27. X. Qin, Y. Luo, W. Lu, G. Chang, A. M. Asiri, A. O. Al-Youbi and X. Sun, *Electrochim. Acta*, 2012, **79**, 46-51.
28. W. Zhao, H. Wang, X. Qin, X. Wang, Z. Zhao, Z. Miao, L. Chen, M. Shan, Y. Fang and Q. Chen, *Talanta*, 2009, **80**, 1029-1033.
29. E. Kurowska, A. Brzózka, M. Jarosz, G. D. Sulka and M. Jaskuła, *Electrochim. Acta*, 2013, **104**, 439-447.